*J. Fluid Mech.* (1978), *vol.* 86, *part* 2, *pp.* 365–383
*Printed in Great Britain*



# Free convective heat transfer in a viscous incompressible fluid confined between a long vertical wavy wall and a parallel flat wall

By K. VAJRAVELU AND K. S. SASTRI†
Department of Mathematics, Indian Institute of Technolcgy, Kharagpur 721302

(Received 8 August 1977)

Analyses of fluid flow over a wavy wall are of interest because of their applications to the physical problems mentioned in § 1. The authors have therefore devoted their attention to the effect of waviness of one of the walls on the flow and heat-transfer characteristics of an incompressible viscous fluid confined between two long vertical walls and set in motion by a difference in the wall temperatures. The equations governing the fluid flow and heat transfer have been solved subject to the relevant boundary conditions by assuming that the solution consists of two parts: a mean part and a disturbance or perturbed part. To obtain the perturbed part of the solution use has been made of the long-wave approximation. The mean (zeroth-order) part of the solution has been found to be in good agreement with that of Ostrach (1952) after certain modifications resulting from the different non-dimensionalizations employed by Ostrach and the present authors respectively. The perturbed part of the solution is the contribution from the waviness of the wall. The zeroth-order, the first-order and the total solution of the problem have been evaluated numerically for several sets of values of the various parameters entering the problem. Certain qualitatively interesting properties of the flow and heat transfer, along with the changes in the fluid pressure on the wavy and flat wall, are recorded in §§ 5 and 6.

## 1. Introduction

Viscous fluid flow over a wavy wall has attracted the attention of relatively few researchers although the analysis of such flows finds application in different areas such as transpiration cooling of re-entry vehicles and rocket boosters, cross-hatching on ablative surfaces and film vaporization in combustion chambers. In view of these various applications, Lekoudis, Nayfeh & Saric (1976) have made a linear analysis of compressible boundary-layer flows over a wavy wall. Shankar & Sinha (1976) have made a detailed study of the Rayleigh problem for a wavy wall and arrived at certain interesting conclusions, namely that at low Reynolds numbers the waviness of the wall quickly ceases to be of importance as the liquid is dragged along by the wall, while at large Reynolds numbers the effects of viscosity are confined to a thin layer close to the wall and the known potential solution emerges in time. Lessen & Gangwani (1976) have made a very interesting analysis of the effect of small amplitude wall waviness upon the stability of the laminar boundary layer. In all these studies the authors have

† Present address: Department of Mechanical and Aerospace Engineering, Cornell University, Ithaca, New York 14853.

taken the wavy wall to be oriented in a horizontal direction and studied the effect of the waviness on the flow field.

So far as the present authors are aware, very little attention has been paid to the study of the free convective heat transfer in a viscous fluid flowing over a wavy wall or confined between two walls one or both of which are wavy. The present authors have therefore attempted to tackle this complicated problem of physical interest and to throw light on the effect of the wavy wall on the flow and heat-transfer characteristics in the problem described in the title (the results for the case where both walls are wavy will be discussed in a separate paper). As the problem is highly complicated it has been solved by a linearization technique wherein the solution is made up of two parts: a mean part corresponding to the fully developed mean flow and a small disturbance. It is worth mentioning here that the mean part of the solution coincides with that of Ostrach's (1952) problem after modifications resulting from the different non-dimensionalizations used by Ostrach and the present authors respectively. It should be mentioned here that in obtaining the disturbance part of the solution the authors have used the long-wave approximation. Also, the authors have observed several interesting properties of the flow and heat-transfer characteristics (see § 5).

## 2. Formulation and solution of the problem

Consider the channel shown in figure 1, in which the $X$ axis is taken vertically upwards and parallel to the flat wall while the $Y$ axis is taken perpendicular to it in such a way that the wavy wall is represented by $Y = \epsilon^* \cos KX$ and the flat wall by $Y = d$. The wavy and flat walls are maintained at constant temperatures of $T_w$ and $T_1$ respectively. We make the following assumptions:

(i) that all the fluid properties are constant except the density in the buoyancy-force term;

(ii) that the flow is laminar, steady and two-dimensional;

(iii) that the viscous dissipation and the work done by pressure are sufficiently small in comparison with both the heat flow by conduction and the wall temperatures;

(iv) that the volumetric heat source/sink term in the energy equation is constant;

(v) that the wavelength of the wavy wall, which is proportional to $1/K$, is large.

Under these assumptions, the equations which govern steady two-dimensional flow and heat transfer in a viscous incompressible fluid occupying the channel shown in figure 1 are the momentum equations

$$\rho\left(U\frac{\partial U}{\partial X}+V\frac{\partial U}{\partial Y}\right)=-\frac{\partial P^*}{\partial X}+\mu\left(\frac{\partial^2 U}{\partial X^2}+\frac{\partial^2 U}{\partial Y^2}\right)-\rho g_X, \tag{1}$$

$$\rho\left(U\frac{\partial V}{\partial X}+V\frac{\partial V}{\partial Y}\right)=-\frac{\partial P^*}{\partial Y}+\mu\left(\frac{\partial^2 V}{\partial X^2}+\frac{\partial^2 V}{\partial Y^2}\right), \tag{2}$$

the continuity equation

$$\partial U/\partial X+\partial V/\partial Y=0, \tag{3}$$

and the energy equation

$$\rho C_p\left(U\frac{\partial T}{\partial X}+V\frac{\partial T}{\partial Y}\right)=k\left(\frac{\partial^2 T}{\partial X^2}+\frac{\partial^2 T}{\partial Y^2}\right)+Q, \tag{4}$$

where $U$ and $V$ are the velocity components, $P^*$ is the pressure, $\rho g_X$ is the buoyancy term in the $X$ direction, $Q$ is the constant heat addition/absorption and the other

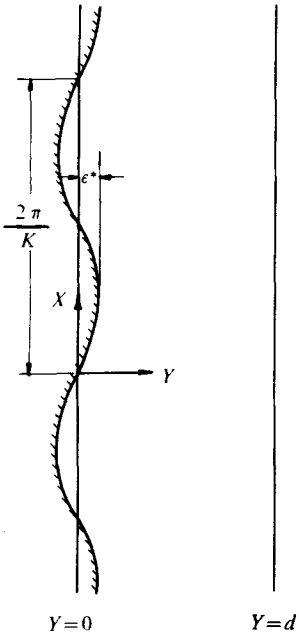


FIGURE 1. Flow configuration.

symbols have their usual meanings. The boundary conditions relevant to the problem are taken as

$$\left.\begin{aligned} &U = 0, \quad V = 0, \quad T = T_w \quad \text{on} \quad Y = \epsilon^* \cos KX, \\ &U = 0, \quad V = 0, \quad T = T_1 \quad \text{on} \quad Y = d. \end{aligned}\right\} \tag{5}$$

We define the non-dimensional variables as

$$x = X/d, \quad y = Y/d, \quad u = Ud/\nu, \quad v = Vd/\nu,$$

$$\theta = (T - T_s)/(T_w - T_s), \quad \bar{P} = P^*/\rho(\nu/d)^2,$$

where $T_s$ is the fluid temperature in static conditions, and with their help rewrite (1)–(4) and the boundary conditions (5) as

$$u\frac{\partial u}{\partial x} + v\frac{\partial u}{\partial y} = -\frac{\partial \bar{P}}{\partial x} + \frac{\partial^2 u}{\partial x^2} + \frac{\partial^2 u}{\partial y^2} - \frac{\rho g_X d^3}{\rho \nu^2}, \tag{6}$$

$$u\frac{\partial v}{\partial x} + v\frac{\partial v}{\partial y} = -\frac{\partial \bar{P}}{\partial y} + \frac{\partial^2 v}{\partial x^2} + \frac{\partial^2 v}{\partial y^2}, \tag{7}$$

$$\partial u/\partial x + \partial v/\partial y = 0, \tag{8}$$

$$P\left(u\frac{\partial \theta}{\partial x} + v\frac{\partial \theta}{\partial y}\right) = \frac{\partial^2 \theta}{\partial x^2} + \frac{\partial^2 \theta}{\partial y^2} + \alpha, \tag{9}$$

$$\left.\begin{aligned} &u = 0, \quad v = 0, \quad \theta = 1 \quad \text{on} \quad y = \epsilon \cos \lambda x, \\ &u = 0, \quad v = 0, \quad \theta = m \quad \text{on} \quad y = 1, \end{aligned}\right\} \tag{10}$$

where $\alpha = Qd^2/k(T_w - T_s)$, the non-dimensional heat-source/sink parameter,

$P = \mu C_p/k$, the Prandtl number,

$\epsilon = \epsilon^*/d$, the non-dimensional amplitude parameter,

$\lambda = Kd$, the non-dimensional frequency parameter,

$m = (T_1 - T_s)/(T_w - T_s)$, the wall-temperature ratio.

In the static fluid (subscript $s$) we have

$$0 = -\frac{\partial \overline{P}_s}{\partial x} - \frac{\rho_s g_X d^3}{\rho \nu^2}. \tag{11}$$

In view of (11), (6) becomes

$$u\frac{\partial u}{\partial x} + v\frac{\partial u}{\partial y} = -\frac{\partial(\overline{P} - \overline{P}_s)}{\partial x} + \frac{\partial^2 u}{\partial x^2} + \frac{\partial^2 u}{\partial y^2} + G\theta, \tag{12}$$

where $(\rho - \rho_s)/\rho = -\beta(T_w - T_s)\theta$ is the well-known Boussinesq approximation and $G = d^3 g_X \beta(T_w - T_s)/\nu^2$, the Grashof number or free-convection parameter. By the method of perturbations let us take the flow field and the temperature field to be

$$\left.\begin{aligned} u(x,y) &= u_0(y) + u_1(x,y), \quad v(x,y) = v_1(x,y), \\ \overline{P}(x,y) &= P_0(x) + P_1(x,y), \quad \theta(x,y) = \theta_0(y) + \theta_1(x,y), \end{aligned}\right\} \tag{13}$$

where the perturbations $u_1, v_1, P_1$ and $\theta_1$ are small compared with the mean or the zeroth-order quantities. With the help of (13), equations (12) and (7)–(9) become

$$d^2u_0/dy^2 + G\theta_0 = C, \quad d^2\theta_0/dy^2 = -\alpha \tag{14}$$

to zeroth order and

$$u_0\frac{\partial u_1}{\partial x} + v_1\frac{\partial u_0}{\partial y} = -\frac{\partial P_1}{\partial x} + \frac{\partial^2 u_1}{\partial x^2} + \frac{\partial^2 u_1}{\partial y^2} + G\theta_1, \tag{15}$$

$$u_0\frac{\partial v_1}{\partial x} = -\frac{\partial P_1}{\partial y} + \frac{\partial^2 v_1}{\partial x^2} + \frac{\partial^2 v_1}{\partial y^2}, \tag{16}$$

$$\partial u_1/\partial x + \partial v_1/\partial y = 0, \tag{17}$$

$$P\left(u_0\frac{\partial \theta_1}{\partial x} + v_1\frac{\partial \theta_0}{\partial y}\right) = \frac{\partial^2 \theta_1}{\partial x^2} + \frac{\partial^2 \theta_1}{\partial y^2} \tag{18}$$

to first order, where $C = \partial(P_0 - P_s)/\partial x$, and is taken equal to zero (see Ostrach 1952). With the help of (13) the boundary conditions (10) can be easily simplified to

$$\left.\begin{aligned} u_0 &= 0, \quad \theta_0 = 1 \quad \text{on} \quad y = 0, \\ u_0 &= 0, \quad \theta_0 = m \quad \text{on} \quad y = 1, \end{aligned}\right\} \tag{19}$$

$$\left.\begin{aligned} u_1 &= -u_0', \quad v_1 = 0, \quad \theta_1 = -\theta_0' \quad \text{on} \quad y = 0, \\ u_1 &= 0, \quad v_1 = 0, \quad \theta_1 = 0 \quad \text{on} \quad y = 1, \end{aligned}\right\} \tag{20}$$

where a prime denotes differentiation with respect to $y$.

Introducing the stream function $\overline{\psi}_1$ defined by

$$u_1 = -\partial\overline{\psi}_1/\partial y, \quad v_1 = \partial\overline{\psi}_1/\partial x \tag{21}$$

(from which we infer that (17) is satisfied identically) into (15), (16) and (18) and eliminating the non-dimensional pressure $P_1$, we get

$$u_0(\overline{\psi}_{1,xxx}+\overline{\psi}_{1,yyy})-\overline{\psi}_{1,x}u_0''=2\overline{\psi}_{1,xxyy}+\overline{\psi}_{1,yyyy}+\overline{\psi}_{1,xxxx}-G\theta_{1,y} \tag{22}$$

and
$$P(u_0\theta_{1,x}+\overline{\psi}_{1,x}\theta_0')=\theta_{1,xx}+\theta_{1,yy}. \tag{23}$$

Assuming
$$\overline{\psi}_1(x,y)=\epsilon\, e^{i\lambda x}\psi(y), \quad \theta_1(x,y)=\epsilon\, e^{i\lambda x}t(y), \tag{24}$$

from which we infer

$$u_1(x,y)=\epsilon\, e^{i\lambda x}\overline{u}_1(y), \quad v_1(x,y)=\epsilon\, e^{i\lambda x}\overline{v}_1(y),$$

and using (24) in (22) and (23), we get

$$\psi^{iv}-i\lambda[u_0(-\lambda^2\psi+\psi'')+u_0''\psi]-\lambda^2(2\psi''-\lambda^2\psi)=Gt' \tag{25}$$

and
$$t''-\lambda^2 t=Pi\lambda(u_0t+\psi\theta_0'). \tag{26}$$

Below we restrict our attention to the real parts of the solutions for the perturbed quantities $\overline{\psi}_1$, $\theta_1$, $u_1$ and $v_1$ and write the real part of a quantity $F$ as $\mathrm{Re}\,F$.

The boundary conditions (20) can be now written in terms of $\overline{\psi}_1$ as

$$\left.\begin{aligned}&\partial\overline{\psi}_1/\partial y=u_0', \quad \partial\overline{\psi}_1/\partial x=0 \quad \text{on} \quad y=0,\\ &\partial\overline{\psi}_1/\partial y=0, \quad \partial\overline{\psi}_1/\partial x=0 \quad \text{on} \quad y=1.\end{aligned}\right\} \tag{27}$$

If we consider small values of $\lambda$ (or $K\ll 1$) then substituting

$$\psi(\lambda,y)=\sum_i\lambda^i\psi_i, \quad t(\lambda,y)=\sum_i\lambda^i t_i \quad (i=0,1,2,\ldots)$$

into (25), (26) and (27) gives, to order of $\lambda^2$, the following sets of ordinary differential equations and corresponding boundary conditions:

$$\psi_0^{iv}=Gt_0, \quad t''=0, \tag{28}$$

$$\left.\begin{aligned}&\psi_1^{iv}+iu_0''\psi_0-iu_0\psi_0''=Gt_1',\\ &t_1'=Pi(u_0t_0+\psi_0\theta_0'),\end{aligned}\right\} \tag{29}$$

$$\left.\begin{aligned}&\psi_2^{iv}=i(u_0''\psi_1-u_0\psi_1'')-2\psi_0''=Gt_2',\\ &t_2''=Pi(u_0t_1+\psi_1\theta_0')+t_0\end{aligned}\right\} \tag{30}$$

and
$$\left.\begin{aligned}&\psi_0'=u_0', \quad \psi_0=0, \quad t_0=-\theta_0' \quad \text{on} \quad y=0,\\ &\psi_0'=0, \quad \psi_0=0, \quad t_0=0 \quad\quad \text{on} \quad y=1,\end{aligned}\right\} \tag{31}$$

$$\left.\begin{aligned}&\psi_i'=0, \quad \psi_i=0, \quad t_i=0 \quad \text{on} \quad y=0\\ &\psi_i'=0, \quad \psi_i=0, \quad t_i=0 \quad \text{on} \quad y=1\end{aligned}\right\} \quad \text{for} \quad i\geqslant 1. \tag{32}$$

*Zeroth-order solution (mean part)*

The solutions for the zeroth-order velocity $u_0$ and the zeroth-order temperature $\theta_0$ satisfying the differential equations (14) and the boundary conditions (19) have been obtained but are not presented here for the sake of brevity. The expressions for $u_0$ and $\theta_0$ at various values of $y$ have been evaluated numerically for several sets of values of the parameters $G$, $m$ and $\alpha$. Some of the qualitatively interesting properties of $u_0$ and $\theta_0$ are presented in figures 2 and 3.

*Skin friction and heat-transfer coefficient (Nusselt number) at the walls*

The shear stress $\tau_{xy}$ at any point in the fluid is given by $\tau_{xy} = \mu(\partial U/\partial Y + \partial V/\partial X)$. In dimensionless form this becomes $\tau_{xy} = d^2\tau_{xy}/\rho\nu^2 = \partial u/\partial y + \partial v/\partial x$. At the wavy wall $y = \epsilon\cos\lambda x$ and at the flat wall $y = 1$, $\tau_{xy}$ becomes

$$\tau_w = \tau_0^0 + \mathrm{Re}\,[\epsilon e^{i\lambda x} u_0''(0) + \epsilon e^{i\lambda x}\bar{u}_1'(0)] \tag{33}$$

and

$$\tau_1 = \tau_1^0 + \mathrm{Re}\,[\epsilon e^{i\lambda x}\bar{u}_1'(1)] \tag{34}$$

respectively, where

$$\tau_0^0 = u_0'(0) \quad \text{and} \quad \tau_1^0 = u_0'(1). \tag{35}$$

In a similar way the heat-transfer coefficient $h$ is defined as $h = -k\,\partial T/\partial Y$, which in non-dimensional form becomes

$$h = -k\frac{(T_w - T_s)}{d}\left[\frac{d\theta_0}{dy} + \mathrm{Re}\left(\epsilon e^{i\lambda x}\frac{d\theta_1}{dy}\right)\right],$$

or

$$Nu = -\frac{dh}{T_w - T_s} = \theta_0'(y) + \mathrm{Re}\,[\epsilon e^{i\lambda x}\theta_1'(y)]. \tag{36}$$

At the wavy wall $y = \epsilon\cos\lambda x$ and the flat wall $y = 1$, (36) takes the forms

$$Nu_w = Nu_0^0 + \mathrm{Re}\,[\epsilon e^{i\lambda x}\theta_0''(0) + \epsilon e^{i\lambda x}\theta_1'(0)] \tag{37}$$

and

$$Nu_1 = Nu_1^0 + \mathrm{Re}\,[\epsilon e^{i\lambda x}\theta_1'(1)] \tag{38}$$

respectively, where

$$Nu_0^0 = \theta_0'(0) \quad \text{and} \quad Nu_1^0 = \theta_0'(1). \tag{39}$$

The expressions for $\tau_{0,1}^0$ and $Nu_{0,1}^0$ have been obtained from the zeroth-order solutions $u_0$ and $\theta_0$ and have been evaluated numerically for several sets of values of the parameters $G$, $m$ and $\alpha$. It is clear that expressions (35) and (39) are the zeroth-order skin friction and zeroth-order heat-transfer coefficient at the walls and that their numerical values correspond physically to the behaviour of the flow and heat transfer at the walls in the case of a channel whose walls are both flat (Ostrach's (1952) problem).

## 3. Discussion of the zeroth-order solutions

The results in figures 2–5 are naturally applicable to the case of a channel both of whose walls are flat; this problem was discussed by Ostrach (1952), both with and without the frictional heating terms taken into account. As the non-dimensionalization used by Ostrach is different from that used in the present analysis, it is worth repeating here the salient features of the flow and heat-transfer characteristics to aid comparison of the present results with those for a flat-walled channel.

We notice from the differential equations (14) that the non-dimensional (zeroth-order) temperature of the fluid is affected only by the heat-source parameter $\alpha$ and the wall-temperature ratio $m$ and that the non-dimensional velocity of the fluid is affected by the free-convection parameter $G$ in addition to the parameters $\alpha$ and $m$.

The behaviour of the non-dimensional zeroth-order velocity $u_0$ of the fluid with changes in the free-convection parameter $G$ and the heat-source parameter $\alpha$ is depicted in figure 2(*a*) for the case $m = -1$ (physically, $m = -1$ means that the

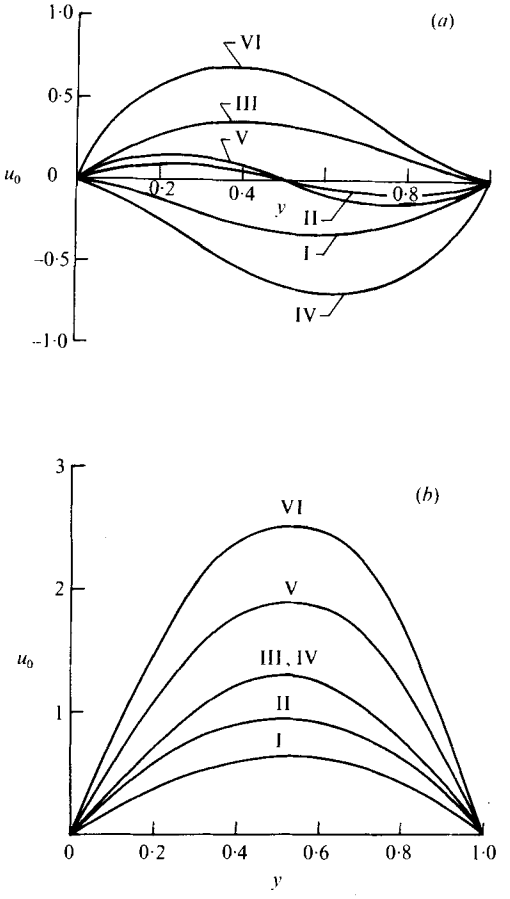


FIGURE 2. Dimensionless zeroth-order velocity profiles. (*a*) $m = -1$. (*b*) $m = 2$.

| | I | II | III | IV | V | VI |
|---|---|---|---|---|---|---|
| $G$ | 5 | 5 | 5 | 10 | 10 | 10 |
| $\alpha$ | −5 | 0 | 5 | −5 | 0 | 5 |

average of the temperatures of the two walls is equal to that of the static fluid) and in figure 2(*b*) for $m = 2$ (wall temperatures unequal). From figure 2(*a*), it is clear that, with an increase in the free-convection parameter $G$, the magnitude of the fluid velocity $u_0$ increases across the entire channel width but the shape of the curve $u_0$ *vs.* $y$ remains unchanged in each case, including $\alpha = 0$ (no heat sources or sinks, curves II and V). Thus in the presence of heat sources ($\alpha > 0$, curves III and VI) the fluid velocity increases across the channel width whenever the free-convection parameter $G$ increases and this behaviour is reversed in the case of heat sinks ($\alpha < 0$, curves I and IV). On fixing $G$ and varying $\alpha$ we observe that with an increase in the heat-source parameter $\alpha$ the fluid velocity increases considerably.

From figure 2(*b*), it is obvious that for $m = 2$ the fluid velocity $u_0$ is enhanced by an increase in the free-convection parameter $G$ for all values of $\alpha$. Qualitatively similar behaviour of the fluid velocity occurs with an increase in $\alpha$ (curves I, II, III). The conclusions drawn for the fluid velocity in the case of unequal wall temperatures ($m = 2$) hold qualitatively for the case of equal wall temperatures ($m = 1$), the results

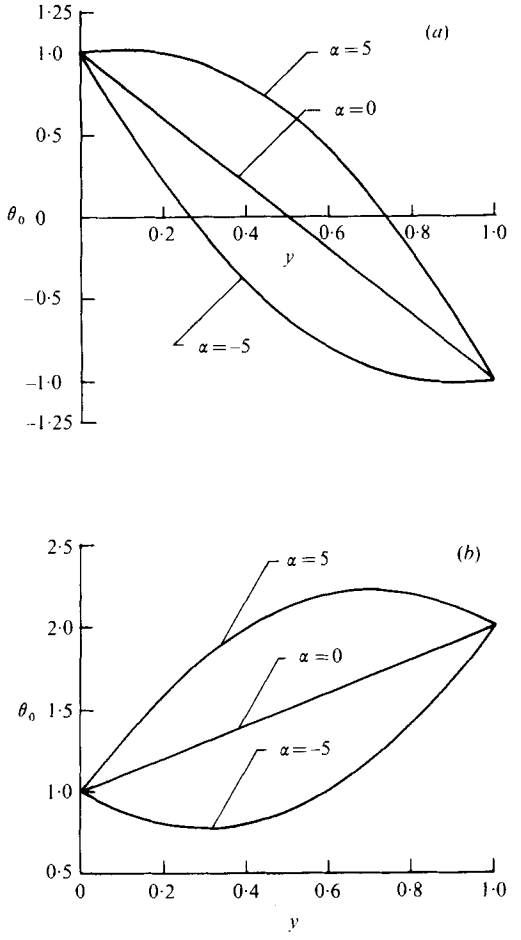


FIGURE 3. Dimensionless zeroth-order temperature profiles. (*a*) $m = -1$. (*b*) $m = 2$.

for which are therefore not presented in the figures. Close examination of figures 2(*a*) and (*b*) reveals that the fluid velocity can reverse its direction in the case $m = -1$ while there is no such possibility when $m \geqslant 0$. Physically, this can be ascribed to the fact that, for $m \geqslant 0$, while the temperature of one wall exceeds that of the static fluid, the temperature of the other wall lies below that of the static fluid.

The behaviour of the fluid temperature with changes in $\alpha$ is shown for $m = -1$ in figure 3(*a*) and for $m = 2$ in figure 3(*b*). From figure 3(*a*) it is clear that in the absence of heat sources the fluid temperature $\theta_0$ is a linearly decreasing function of $y$ while in the presence of heat sources ($\alpha = 5 > 0$) the temperature is parabolic in nature [see (14)], increasing from its value at the wall $y = 0$ to a maximum temperature at around $y = 0{\cdot}1$ and then decreasing steadily to its value at $y = 1$. In the presence of heat sinks ($\alpha = -5 < 0$) the behaviour of the fluid temperature is the exact opposite of that observed in the case of heat sources ($\alpha > 0$). From figure 3(*b*) it is clear that when $m = 2$ the fluid temperature $\theta_0$ increases with $\alpha$. In the absence of heat sources ($\alpha = 0$) the fluid temperature increases linearly when $m = 2$ unlike the case $m = -1$, the results for $\alpha \neq 0$ being the same.

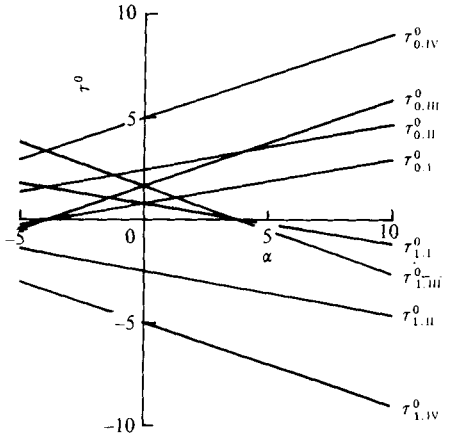


FIGURE 4. Zeroth-order skin friction at $y = 0$ and $y = 1$.

| | I | II | III | IV |
|---|---|---|---|---|
| $G$ | 5 | 5 | 10 | 10 |
| $m$ | −1 | 1 | −1 | 1 |

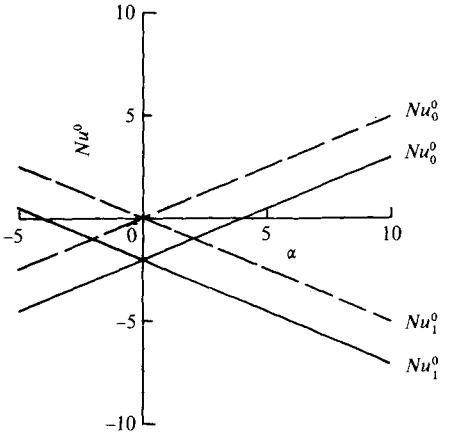


FIGURE 5. Zeroth-order Nusselt numbers at $y = 0$ and $y = 1$.
——, $m = -1$; – – –, $m = 1$.

Figure 4 shows that the zeroth-order skin friction at either wall is a linear function of the heat-source parameter $\alpha$ and that the skin friction at the wall $y = 0$ increases with the heat-source parameter while the reverse is true at the other wall ($y = 1$). The skin friction at $y = 0$, in general, is an increasing function of the free-convection parameter $G$ while that at $y = 1$ decreases with an increase in $G$, this behaviour holding for any value of the wall-temperature ratio $m$. On fixing $G$ and changing $m$ we notice from figure 4 that the skin friction at $y = 0$ increases with $m$ while that at the other wall decreases (I, II, or III, IV), a result qualitatively similar to the effect of $G$.

The heat-transfer coefficient $Nu^0$ increases with increasing $\alpha$ at $y = 0$ and decreases at the other wall for all values of $m$ (see figure 5). Also the rate of heat transfer at either wall increases with an increase in $m$. But its value at $y = 0$ ($y = 1$) generally changes sign from negative (positive) to positive (negative) when the heat-source

parameter takes higher and higher values (see figure 5), a result physically equivalent to saying that heat can sometimes flow out of and at other times into either wall. Finally we mention that all the foregoing conclusions on the behaviour of the flow and heat-transfer characteristics agree qualitatively with those of Ostrach (1952).

## 4. Calculation of first-order quantities

*Velocities and temperature*

The sets of equations (28)–(30), subject to the boundary conditions (31) and (32), have been solved exactly for $\psi_i$ and $t_i$ ($i = 0, 1, 2$). The expressions

$$\psi = \sum_{i=0}^{2} \lambda^i \psi_i, \quad t = \sum_{i=0}^{2} \lambda^i t_i \tag{40}$$

have been used along with (24) and (21) to calculate the expressions for the perturbed quantities $u_1$, $v_1$ and $\theta_1$, which after obvious simplifications take the form

$$\left.\begin{aligned} u_1 &= -\epsilon[\cos(\lambda x)\,\psi_r' - \sin(\lambda x)\,\psi_i'], \\ v_1 &= -\epsilon\lambda[\sin(\lambda x)\,\psi_r + \cos(\lambda x)\,\psi_i], \\ \theta_1 &= \epsilon[\cos(\lambda x)\,t_r - \sin(\lambda x)\,t_i], \end{aligned}\right\} \tag{41}$$

where

$$\left.\begin{aligned} \psi_r + i\psi_i = \psi, \quad \psi_r' + i\psi_i' = \psi', \\ t_r + it_i = t, \quad t_r' + it_i' = t'. \end{aligned}\right\} \tag{42}$$

The expressions for $u_1$, $v_1$ and $\theta_1$ are called the first-order solutions or the disturbed parts. In a similar way, from (13) the total (dimensionless) velocity field $(u, v)$ and the total (dimensionless) temperature field $\theta$ have been obtained but for the sake of brevity are not presented here. For several sets of values of the non-dimensional parameters $G$, $\lambda$, $m$, $\alpha$, $\epsilon$ and $P$, the expressions for $(u_1, v_1, \theta_1)$, $(u, v, \theta)$, the wall skin friction $\tau_{w,1}$ and the wall Nusselt number $Nu_{w,1}$ [see (33), (34), (37) and (38)] have been calculated numerically. Some of their interesting features are presented in figures 6–11.

*Pressure drop*

We refer to (6) and (7) and obtain the fluid pressure $\bar{P}(x, y)$ (note that $P_0(x) =$ constant) at any point $(x, y)$ as

$$\bar{P}(x, y) = \int d\bar{P} = \int \left[\frac{\partial \bar{P}}{\partial x}\,dx + \frac{\partial \bar{P}}{\partial y}\,dy\right],$$

i.e.

$$\bar{P}(x, y) - L = \mathrm{Re}\left[\epsilon \frac{\exp(i\lambda x_i)}{\lambda}\, iZ(y)\right], \tag{43}$$

where $L$ is an arbitrary constant and

$$Z(y) = (\psi''' - \lambda^2\psi') - i\lambda(u_0\psi' - u_0'\psi) - Gt.$$

Equation (43) can be rewritten as

$$\hat{P} = \bar{P}(x, y) - \bar{P}(x, 1) = (\epsilon/\lambda)\,\mathrm{Re}\,[i\,e^{i\lambda x}(Z(y) - Z(1)], \tag{44}$$

where $\hat{P}$ has been named the pressure drop since it indicates the difference between the pressure at any point $y$ in the flow field and that at the flat wall, with $x$ fixed. The

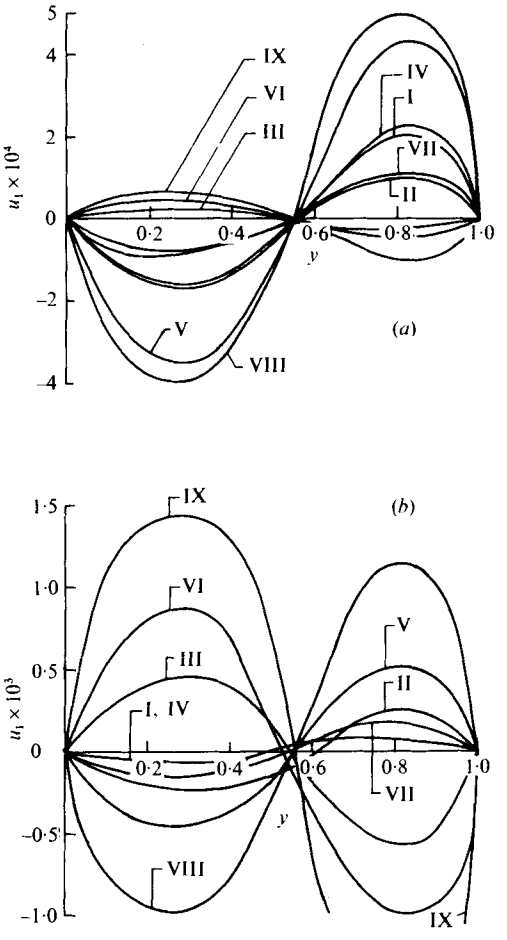


FIGURES 6 (*a*, *b*). For legend see next page.

pressure drops $\hat{P}$ at $\lambda x = 0$ and $\frac{1}{2}\pi$ have been named $\hat{P}_0$ and $\hat{P}_{\frac{1}{2}\pi}$ and their numerical values for several sets of values of the non-dimensional parameters $G, \lambda, m, \epsilon, \alpha, P$ and $y$ have been evaluated and are presented in figure 12. In what follows we record the qualitative differences in the behaviour of the various flow and heat-transfer characteristics which show clearly the effects of the wavy wall of the channel under consideration.

## 5. Discussion of the first-order solution, the total solution and the pressure drop

Figures 6 and 7 depict the behaviour of the perturbed (first-order solution) quantities $u_1, v_1$ and $\theta_1$ when $m = -1$ and when the Prandtl number is 0·71 and 7. From figure 6 (*a*) we observe that in the presence of heat sources the fluid velocity $u_1$ increases steadily for a fixed $y$ up to $y = 0{\cdot}55$ approximately, i.e. in the first half of the channel, while in the other half $u_1$ is a decreasing function of $y$. We notice further that when $\alpha > 0$ (curves III, VI of figure 6*a*) an increase in the frequency parameter $\lambda$ increases the

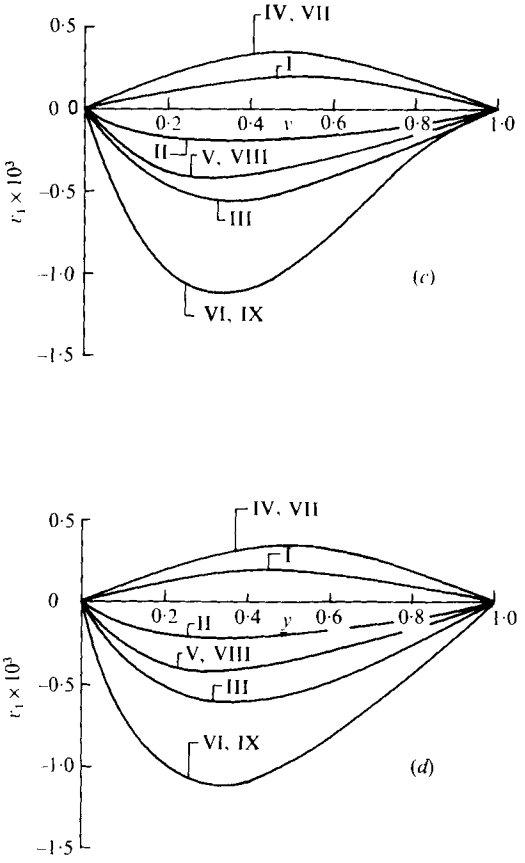


FIGURE 6. Dimensionless first-order velocity profiles. $m = -1$. (*a*), (*c*) $P = 0{\cdot}71$. (*b*), (*d*) $P = 7$.

| | I | II | III | IV | V | VI | VII | VIII | IX |
|---|---|---|---|---|---|---|---|---|---|
| $G$ | 5 | 5 | 5 | 5 | 5 | 5 | 10 | 10 | 10 |
| $\lambda$ | 0·01 | 0·01 | 0·01 | 0·02 | 0·02 | 0·02 | 0·01 | 0·01 | 0·01 |
| $\alpha$ | −5 | 0 | 5 | −5 | 0 | 5 | −5 | 0 | 5 |

fluid velocity $u_1$ in the first half of the channel considerably and that this behaviour is reversed when $\alpha \leqslant 0$ (see curves II, V and I, IV). This behaviour is reversed in the other half of the channel. It is worth mentioning that, in the first half of the channel, an increase in the free-convection parameter $G$ tends to increase the fluid velocity $u_1$ significantly when the heat-source parameter $\alpha$ is positive or negative (III, IX and I, VII) while it decreases the fluid velocity $u_1$ in the absence of heat sources ($\alpha = 0$; II, VIII). However in the other half this behaviour of the fluid velocity $u_1$ with $G$ is reversed. All the above results hold qualitatively in the case of water ($P = 7$; see figure 6*b*) as well as in the case of air ($P = 0{\cdot}71$) but the magnitudes of the increases or decreases in the velocity $u_1$ of air in figure 6(*a*) are changed considerably in the case of water.

Figures 6(*c*) and (*d*) show the behaviour of the fluid velocity $v_1$ perpendicular to the channel length. From curves I, II and III in figure 6(*c*), we notice that as the heat-source parameter $\alpha$ is increased the velocity $v_1$ diminishes sharply. Also, the effect of

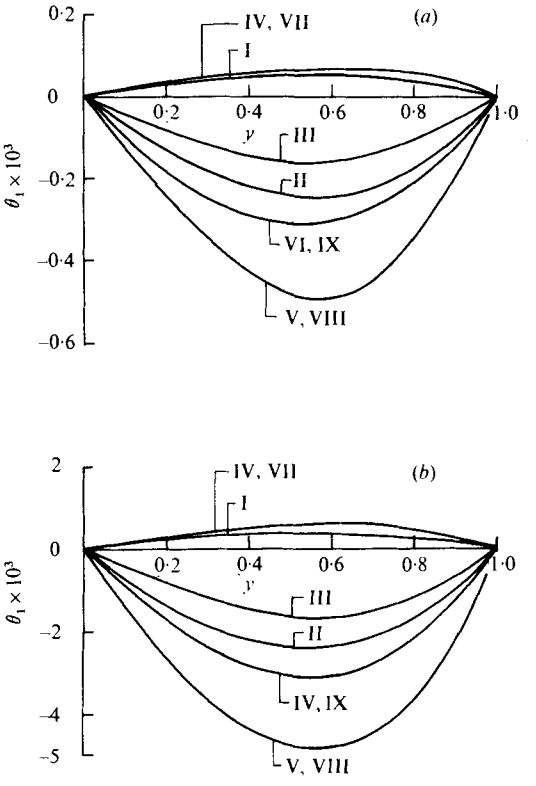


FIGURE 7. Dimensionless first-order temperature profiles. $m = -1$.
(*a*) $P = 0{\cdot}71$. (*b*) $P = 7$. Curves as in figure 6.

an increase in the frequency parameter $\lambda$ is to reduce the velocity $v_1$ when $\alpha \geqslant 0$ and to enhance it when $\alpha < 0$. We observe further from figure 6 (*c*) that the effect of the free-convection parameter $G$ on the velocity $v_1$ is qualitatively similar to that of the frequency parameter $\lambda$. The above observations for the fluid velocity $v_1$ hold qualitatively in the case of water ($P = 7$) as well as in the case of air ($P = 0{\cdot}71$) (compare figures 6*c*, *d*).

From figures 7 (*a*) and (*b*) we can make out the behaviour of the fluid temperature $\theta_1$ in the cases of air and water respectively. After a keen perusal of figures 7 (*a*) and (*b*) and comparing them with figures 6 (*c*) and (*d*) we arrive at the striking conclusion that the variation with each of the parameters $G$, $\lambda$ and $\alpha$ of the fluid temperature $\theta_1$, be it for air or for water, resembles that of the velocity $v_1$.

Figures 8 (*a*) and (*b*) describe the behaviour of the total fluid velocity $u$ ($= u_0 + u_1$) when the wall temperature ratio $m$ is $-1$ and 2, respectively, in the case of air only. Increasing values of the heat-source parameter $\alpha$ enhance the total velocity $u$ considerably both when $m = -1$ and when $m = 2$. The effects of the free-convection parameter $G$ and the frequency parameter $\lambda$ on the total velocity $u$ are very similar when $m = -1$. Again, when $m = -1$ and the heat-source parameter $\alpha$ is negative, the total velocity $u$ is a decreasing function of both $\lambda$ and $G$ while when $\alpha \geqslant 0$ it increases with both $\lambda$ and $G$. However when $m = 2$, the total velocity $u$ is always an increasing function of both $G$ and $\lambda$ for all values of $\alpha$. It is worth mentioning that of all the

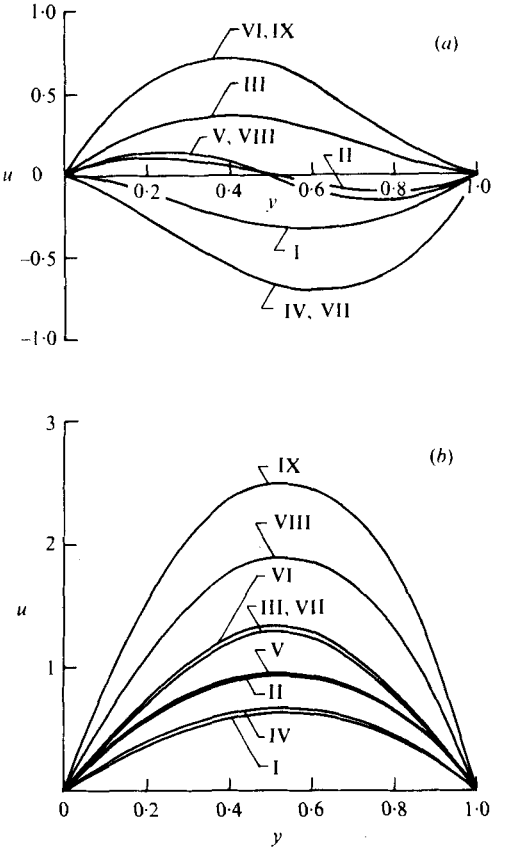


FIGURE 8. Dimensionless velocity profiles. $P = 0{\cdot}71$. (*a*) $m = -1$. (*b*) $m = 2$. Curves as in figure 6.

parameters considered in the problem the effects of $G$ and $m$ on the fluid velocity $u$ are the strongest.

Figures 9(*a*) and (*b*) show the behaviour of the total temperature for air when $m = -1$ and 2 respectively. In these figures the temperature $\theta$ increases significantly with $\alpha$. When $m = -1$ the effect of an increase in $G$ on the temperature $\theta$ is to increase it when $\alpha < 0$ and to diminish it when $\alpha > 0$, the reverse being the case when $m = 2$. We notice further from figure 9 that the effect of the frequency parameter $\lambda$ on the fluid temperature $\theta$ is qualitatively similar to that of the free-convection parameter $G$.

Figure 10 shows the behaviour of the skin friction at the channel walls. When $m = 1$, the skin friction $\tau_w$ at the wavy wall increases with $G$, $P$, $\lambda$ and $\alpha$, the increase with $G$ being the greatest. This behaviour is reversed at the other wall. These conclusions for $m = 1$ hold, more or less, in the case $m = -1$ also. Figure 11 depicts the behaviour of the wall heat-transfer coefficient (the Nusselt number). When $m = 1$, the heat-transfer coefficient at the wavy wall increases with $\alpha$, $\lambda$, or $P$, and $G$, this increase being least significant for $G$ and most significant for $\alpha$. This behaviour is reversed at the flat wall. These conclusions for $m = 1$ hold, more or less, for the case $m = -1$ too. Also, when the heat-source parameter $\alpha$ takes positive increasing values the heat-transfer coefficient at the wavy wall becomes positive and that at the other

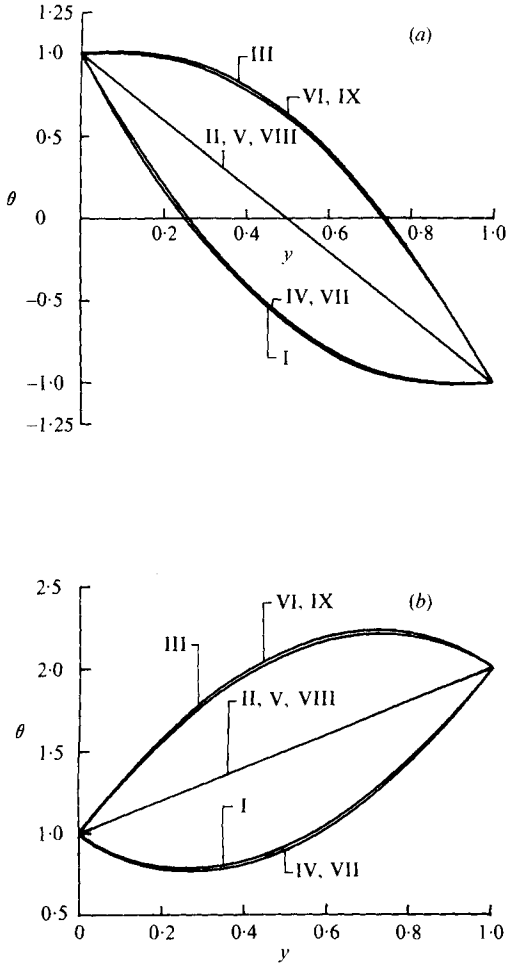


FIGURE 9. Dimensionless temperature profiles. $P = 0{\cdot}71$. (*a*) $m = -1$. (*b*) $m = 2$. Curves as in figure 6.

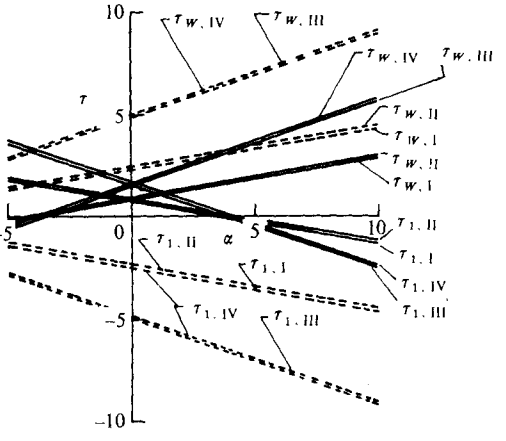


FIGURE 10. Skin friction at the walls. ——, $m = -1$; – – –, $m = 1$.

| | I | II | III | IV |
|---|---|---|---|---|
| $G$ | 5 | 5 | 10 | 10 |
| $\lambda$ | 0·01 | 0·02 | 0·01 | 0·01 |
| $P$ | 0·71 | 0·71 | 0·71 | 7 |

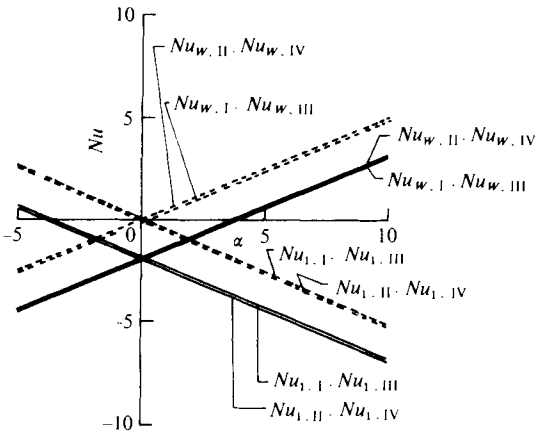


FIGURE 11. Nusselt numbers at the walls. Curves as in figure 10.

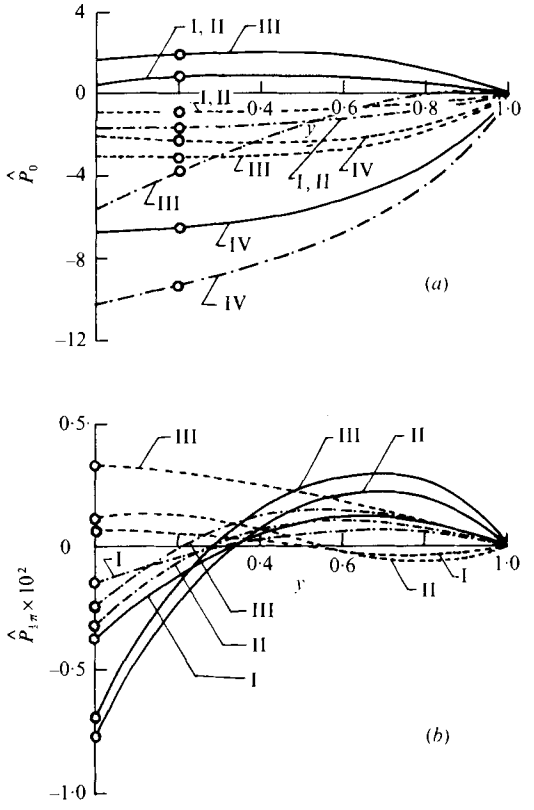


FIGURES 12(*a*, *b*). For legend see facing page.

wall negative, which means physically that heat flows into the walls only. However when the heat-source parameter $\alpha$ takes negative increasing values the heat-transfer coefficient at the wavy wall is negative and that at the other wall positive, which indicates physically that in this case heat flows from the walls into the fluid. These observations hold both when $m = -1$ and when $m = 1$.

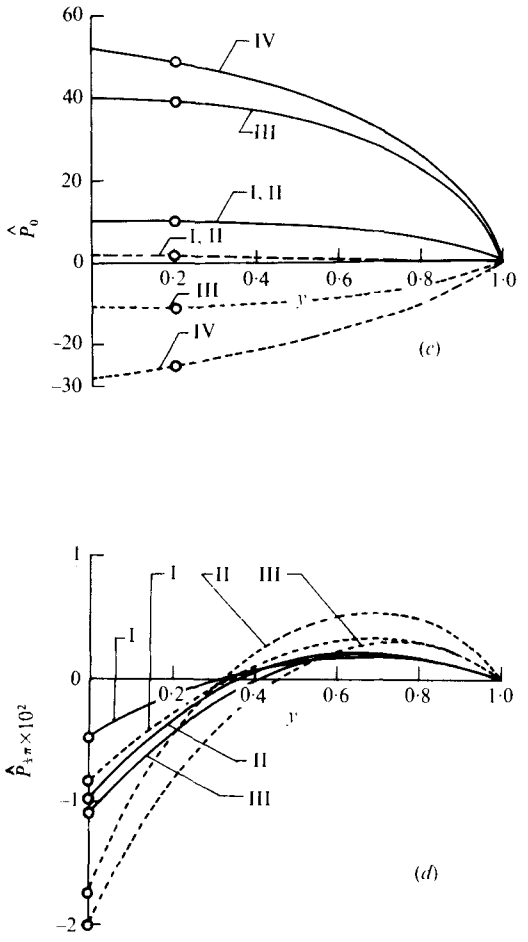


FIGURE 12. Pressure-drop profiles. Curves I–IV as in figure 10. (*a*), (*b*) $m = -1$; – – –, $\alpha = -5$; –·–, $\alpha = 0$; ——, $\alpha = 5$. (*c*), (*d*) $m = 2$; – – –, $\alpha = -5$; ——, $\alpha = 5$.

The behaviour of the pressure drops $\hat{P}_0$ and $\hat{P}_{\frac{1}{2}\pi}$ at $\lambda x = 0$ and $\lambda x = \frac{1}{2}\pi$ are shown in figures 12(*a*) and (*b*) for $m = -1$ and in figures 12(*c*) and (*d*) for $m = 2$. When $\alpha \neq 0$ the pressure drop $\hat{P}_0$ decreases as $G$ increases and increases with $P$ and $\lambda$, while when $\alpha = 0$, $\hat{P}_0$ is a decreasing function of $G$, $\lambda$ and $P$. We may mention, however, that the increase or decrease in $\hat{P}_0$ with increasing $\lambda$ is almost insignificant. The circles in figure 12(*a*) indicate the changes in the fluid pressure on the wavy wall as compared with that on the flat wall. After a keen perusal of the curves in figure 12(*a*) we conclude that the fluid pressure on the wavy wall exceeds that on the flat wall only when $\alpha$ is positive and when $P = 0{\cdot}71$, and that in all other cases considered the fluid pressure on the wavy wall falls below that on the flat wall.

From figure 12(*b*) we see that the pressure drop $\hat{P}_{\frac{1}{2}\pi}$ increases with $G$ and $\lambda$ whether heat sources are present or not. The circles in figure 12(*b*) show, as in figure 12(*a*), the differences between the fluid pressure on the wavy wall and that on the flat wall. In figure 12(*b*), unlike figure 12(*a*), the fluid pressure on the wavy wall, in general, is negative except when $\alpha$ is negative ($\alpha = -5$), which means physically that, in this case only, the fluid pressure on the wavy wall exceeds that on the flat wall.

Figures 12(*c*) and (*d*) show the behaviour of $\hat{P}_0$ and $\hat{P}_{\frac{1}{2}\pi}$ when $m = 2$. The effect of an increase in $G$, $\lambda$ or $P$ is to decrease $\hat{P}_0$ when $\alpha < 0$ and vice versa when $\alpha > 0$. Of the three parameters $G$, $\lambda$ and $P$, the effect of $\lambda$ on $\hat{P}_0$ is the most significant. On looking closely at figure 12(*c*), we observe that when $\alpha$ is negative and the other parameters take higher values the fluid pressure on the wavy wall lies below that on the flat wall and that in all other cases this phenomenon is reversed. From figure 12(*d*) we see that in general the pressure drop $\hat{P}_{\frac{1}{2}\pi}$ decreases significantly as either $G$ or $\lambda$ increases and increases considerably with $\alpha$. It is worth mentioning that in this figure we find the pressure drop on the wavy wall always to be negative, an indication that there is no chance for the fluid pressure on the wavy wall to exceed that on the flat wall.

## 6. Conclusions

We summarize below some of the very interesting properties of the flow and heat transfer in the problem under consideration.

(i) Whether the Prandtl number is small or large, in the first half of the channel ($0 \leqslant y \leqslant 0{\cdot}55$) the effect of an increase in the frequency parameter $\lambda$ on the first-order velocity $u_1$ is to increase it significantly in the presence of heat sources ($\alpha > 0$) and to diminish it considerably in either the absence of heat sources ($\alpha = 0$) or the presence of heat sinks ($\alpha < 0$). This situation is reversed in the other half of the channel. The effect of the free-convection parameter $G$ on the first-order velocity $u_1$ is qualitatively similar to that of the frequency parameter $\lambda$.

(ii) For all Prandtl numbers, the effect of an increase in the frequency parameter $\lambda$ is to diminish the first-order velocity $v_1$ when $\alpha \geqslant 0$. The effect of the free-convection parameter $G$ on the first-order fluid velocity $v_1$ is again similar to that of $\lambda$.

(iii) The effect of each parameter ($G$, $\lambda$, or $P$ or $\alpha$) on the first-order fluid temperature $\theta_1$ is similar in nature to that on the fluid velocity $v_1$. This result and (i) and (ii) also hold when the average of the wall temperatures equals the static temperature.

(iv) When the wall temperatures are unequal ($m = 2$) the total fluid velocity $u$ is always an increasing function of $G$ and $\lambda$ for all values of $\alpha$. When $m = 2$, the total fluid temperature $\theta$ decreases in the presence of heat sinks ($\alpha < 0$) and increases significantly when $\alpha \geqslant 0$ as the free-convection parameter $G$ increases. This behaviour of $\theta$ with $G$ holds qualitatively, more or less, even when the frequency parameter $\lambda$ takes increasing values.

(v) The skin friction at the wavy wall is an increasing function of $G$, $P$, $\lambda$ and $\alpha$, the reverse behaviour occurring at the flat wall. Of all the parameters considered in the problem, the free-convection parameter $G$ has the strongest effect on the skin friction.

(vi) The behaviours of the heat-transfer coefficient at the wavy wall and at the flat wall are qualitatively similar to those of the skin friction at the corresponding walls.

(vii) When the average of the wall temperatures equals that of the static fluid ($m = -1$), the fluid pressure at those points of the wavy wall which correspond to $\lambda x = 0$ exceeds that on the flat wall when $P = 0{\cdot}71$ and heat sources are present, the reverse situation occurring in all other cases. When the wall temperatures are equal and $\alpha = -5$, the fluid pressure on the wavy wall always exceeds that on the flat wall.

(viii) When $m = 2$ and $\lambda x = \frac{1}{2}\pi$, there is no chance for the fluid pressure on the wavy

wall to exceed that on the flat wall, while, when $m = -1$, $\alpha < 0$ and all other parameters take high values, the fluid pressure on the wavy wall lies below that on the flat wall.

The authors take pleasure in recording their gratefulness to IIT Madras for the computer facilities accorded them on the IBM 370 and to IIT Kharagpur for kindly granting permission and sanctioning the requisite funds to allow one of the authors (KV) to go to IIT Madras to carry out the computational work needed in the problem. The authors dedicate this work to Professor B. R. Seth, First Head of Mathematics at IIT Kharagpur, on the occasion of his 71st birthday.

## REFERENCES

LEKOUDIS, S. G., NAYFEH, A. H. & SARIC, W. S. 1976 Compressible boundary layers over wavy walls. *Phys. Fluids* **19**, 514–519.

LESSEN, M. & GANGWANI, S. T. 1976 Effect of small amplitude wall waviness upon the stability of the laminar boundary layer. *Phys. Fluids* **19**, 510–513.

OSTRACH, S. 1952 Laminar natural convection flow and heat transfer of fluids with and without heat sources in channels with constant wall temperature. *N.A.C.A. Tech. Note* no. 2863.

SHANKAR, P. N. & SINHA, U. N. 1976 The Rayleigh problem for a wavy wall. *J. Fluid Mech.* **77**, 243–256.